ENVIRONMENTAL SCIENCE AND POLLUTION SENSING, MONITORING, MODELING AND REMEDIATION

Photocatalysis of fenoxycarb over silver-modified zeolites

**John Ahern · Sofian Kanan · Ziad Sara · Thomas Job ·
Raafat Alnaizy · Nedal Abu Farha · Howard Patterson**

Abstract Two samples of silver doped into zeolite Y were
prepared and characterized. ICP and SEM-EDS analysis indi-
cate that the AgY1 sample contains twice the amount of silver
compared to the AgY2 sample. Solid state luminescence
spectroscopy shows variations in the emission modes of the
site-selective luminescence where various luminophores
might be excited upon selecting the proper excitation energy.
The selected material effectively decomposed the pesticide
fenoxycarb in aqueous solution. The photodecomposition of
fenoxycarb reached 80 % upon irradiation for 60 min in the
presence of the AgY1 catalyst. 2-(4-Phenoxy-phenoxy)ethyl]
carbamic acid (**1**) and 1-amine-2-(phenoxy-4-ol) ethane (**2**)
were identified as products for both uncatalyzed solution and
the catalyzed fenoxycarb with AgY2 catalyst. Whereas, com-
pound (**2**) was the only product identified in the catalyzed
reaction with AgY1.

Keywords Silver · Zeolite · Catalyst · Fenoxycarb ·
Carbamate · Luminescence

J. Ahern · H. Patterson
Department of Chemistry, University of Maine, Orono, ME 04469,
USA

S. Kanan (✉) · Z. Sara · T. Job · N. Abu Farha
Department of Biology, Chemistry & Environmental Sciences,
American University of Sharjah, P.O. Box 26666, Sharjah,
United Arab Emirates
e-mail: skanan@aus.edu

R. Alnaizy
Department of Chemical Engineering, American University of
Sharjah, P.O. Box 26666, Sharjah, United Arab Emirates

Introduction

Insecticides play an important role in protecting food supplies
and reducing the spread of disease. Fenoxycarb (ethyl [2-(4-
phenoxy-phenoxy)ethyl] carbamate) is an example of a
carbamate-type insecticide. It can interrupt insect life cycles,
including inhibition of proper larval development and exten-
sion of seasonal periods of arrest (diapause) (Liu et al. 2008).
Fenoxycarb has been commonly used in crop fields due to its
low toxicity to adult humans and limited persistence in the
environment (Liu et al. 2008). However, it is reported that
fenoxycarb may cause neonatal defects (Oda et al. 2005).
There is also evidence that residues of pesticides on food
including fenoxycarb can be made more bioavailable by the
type of matrix (food) they are in (Payá et al. 2013). This is
made possible by complexes forming with the pesticide and
other compounds that can be more easily absorbed into the
intestine.

Zeolites are aluminosilicate structures commonly used in a
diverse range of applications from cat litter to fuel oil cracking
(Hernández-Maldonado and Yang 2003; Luengnaruemitchai
et al. 2008; Valle et al. 2010; Escola et al. 2011). Numerous
studies have been published by the authors involving zeolite-
assisted photocatalysis of organic pollutants including carba-
mate pesticides (Kanan 2000, 2001; Kanan et al. 2001a, b,
2003a, b, 2006, 2011). The zeolites in these studies are used as
adsorbents for the various pollutants as well as acting as
supports for metal-based photocatalysts that can degrade the
pollutants. One of the most frequently used zeolite
photocatalyst systems is the silver-exchanged faujasite Y ze-
olite. Silver is a popular choice because it can form clusters
within the pores of the zeolite as well as on its surface (Kanan
et al. 2011). Also, silver is chemically stable and can function
as a photocatalyst in natural waters with limited UV light
exposure either from a lamp or a cloudy sky (Kanan et al.
2003a, 2006; Gomez et al. 2011). Faujasite Y zeolite is chosen

for its high surface area and mesoporous structure (Kanan et al. 2003a). Starting with a high surface area, support is especially important because the silver catalyst will fill most pores, thereby providing an environment for silver particles/ions to aggregate and form large sized clusters. The authors have previously used silver-doped Faujasite Y zeolites for the photocatalysis of pesticides including carbaryl (Kanan et al. 2003a, c). The present study focuses on two different AgY zeolites (labeled AgY1 and AgY2) for the photodecomposition of fenoxycarb in distilled water. The AgY2 zeolite has 6.0 % Ag loading by weight and the AgY1 zeolite has 13.7 % which is the maximum loading reached using the method described below. Other than their silver content, the zeolites have the same composition. The properties of the various catalysts are compared against their photocatalytic performance to determine the defining parameters for the degradation of fenoxycarb.

Experimental

Chemicals

Fenoxycarb crystals under normal conditions having a 99.5 % purity were purchased from ChemService. Fenoxycarb solutions were prepared at room temperature in 5:95 methanol/water volume composition. All solvents were high-performance liquid chromatography (HPLC) grade purchased from Aldrich Chemical Company. Silver nitrate and ammonium hydroxide were purchased from Fischer Scientific. Na-Y zeolite was purchased from Fluka. All chemicals were used as received without further purification.

Preparation of AgY samples

Silver clusters were doped in Y zeolite through a cation exchange process. Mixtures with various amounts of silver nitrate solution and ammonia were prepared and digested with NaY zeolite for 24 h at 100 °C. The product was filtered, washed five times with distilled deionized water (ddH$_2$O), and dried at 250 °C for 2 h. Before spectroscopic measurements were taken, the samples were pretreated as follows: degassed at room temperature for 1 h, calcined at 450 K in the presence of 20 Torr of O$_2$ for 1 h, and finally degassed at 450 K for 2 h. The silver loadings were analyzed using an ICP Perkin-Elmer Optima with 1,300 W rf power. The samples were digested as follows: 10 mg of the Ag-zeolite was mixed with 200 μL of 48 % hydrofluoric acid and 200 μL 9 M sulfuric acid. The sample was then diluted to a total volume of 10 mL using ddH$_2$O. The metal-free zeolite was used as a blank. A standard solution of 200 mg/L silver was used to obtain a calibration curve.

Irradiation of the pesticide solutions

Thirty parts per million fenoxycarb solution was prepared in a 5:95 % v/v methanol/water solvent matrix. All solutions were prepared immediately prior to the irradiation experiments and diluted accordingly to obtain the correct solution concentrations in the photochemical reactions. All irradiations were performed using UV lamp which emits a narrow band of irradiation at 254 nm (UV lamps from VWR Scientific, Inc) with a relative intensity of 1,300 μW/cm^2 at 3 in. Each sample was irradiated in quartz test tubes with an inside diameter of 12.5 mm, a length of 10 cm, and 1-mm wall thickness. Only one test tube was irradiated at a time. All solutions were prepared and exposed to UV light at a distance of 3.0 in., where a maximum output of the lamp was reached.

### Low-temperature luminescence measurements

Solid state luminescence measurements of the AgY samples were recorded using QM-1 luminescence spectrometer from Photon Technologies International (PTI) at 77 K. The instrument is equipped with an emission monochromator and double excitation monochromators, a 75-W xenon arc lamp, and a photomultiplier tube serving as the detector. For the luminescence measurements, the samples were made into a pressed pellet and attached to a copper surface. The copper plate was then attached to the transfer tube for the low-temperature experiments. Sequential emission scans were also recorded to form a 3D matrix with excitation as the x axis, emission on the y axis, and intensity on the z axis. The wavelength of the exciting light was run from low to high wavelength at increments of 3 nm between 200 and 500 nm to avoid photobleaching, oxidation, or other forms of degradation.

HPLC and GC-MS analysis

HPLC was used to quantify the irradiated samples from the photolysis experiments. Samples were analyzed with an Agilent 1100 series high-performance liquid chromatograph equipped with an operating software Chemstation for LC 3D with diode array detector. Separations were made on a VYDAC RPC18 column, 250 mm×4.6 mm, 5-μ particle size. Flow rate was 0.5 mL/min for all experiments. The mobile phase used was 60 % acetonitrile and 40 % water. The detector was set to monitor 235 nm.

Gas chromatography-mass spectrometry (GC-MS) measurements were made on a GC-2010 Plus and GCMS-QP2010 Ultra Shimadzu. The mass detector is Electron Ionization Quadropole MS. A 30 m×0.25 mm ID Factor Four VF-5 MS column was used. Components of various samples were separated using the following parameters: injector temperature set at 423 K and detector temperature set at 593 K. The initial oven temperature of 353 K was held for

Fig. 1 SEM images for the two silver zeolite materials **a** AgY1 and **b** AgY2
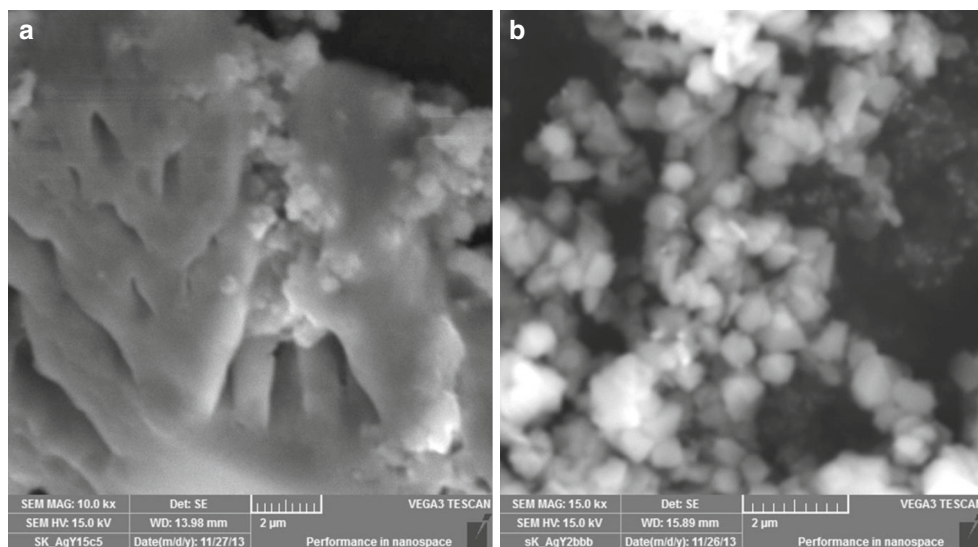
3 min. Then the temperature was ramped to 423 K at a rate of 20 °C/min and held constant for 3 min. Finally, the temperature was ramped to 573 K at the rate of 20 °C/min and held constant for 3 min. Helium was used as the carrier gas with a flow rate of 1 mL/min. Samples were filtered through a Gelman 2-mm Acrodisc® syringe filter previous to injection to remove any particles that may obstruct the column.

SEM-EDS analysis

The SEM images were taken from films that were obtained through casting methodology from suspension of silver zeolite solids in methanol. The images from the films were taken at 23 °C in a Tescan VEGA III LMU scanning electron microscope with Oxford Instrument EDS. The range of accelerating voltage was 0.2–30 kV.

Results and discussion

Silver doped into the framework of zeolite Y was prepared with two different silver contents (labeled as AgY1 and AgY2). ICP analysis shows that the silver contents are 12.0 and 5.5 %, respectively. Figure 1 shows the SEM images for the two silver-doped Y samples and the EDS analysis for various areas result in a silver content of 13.7 and 6.0 %, respectively. As shown in Fig. 1, AgY2 has a well-defined crystalline structure (cubic structure), whereas the AgY1 particles tend to aggregate. In most spots, silver balls/bubbles were identified but directly dispersed by the X-ray beam.

Low-temperature solid-state luminescence revealed distinct high energy (HE) and low energy (LE) emission bands for AgY1 (Fig. 2) and AgY2 (Fig. 3) samples. Excitations were paired to emissions by matching similar peak intensities. The high-energy excitations around 335/337 nm
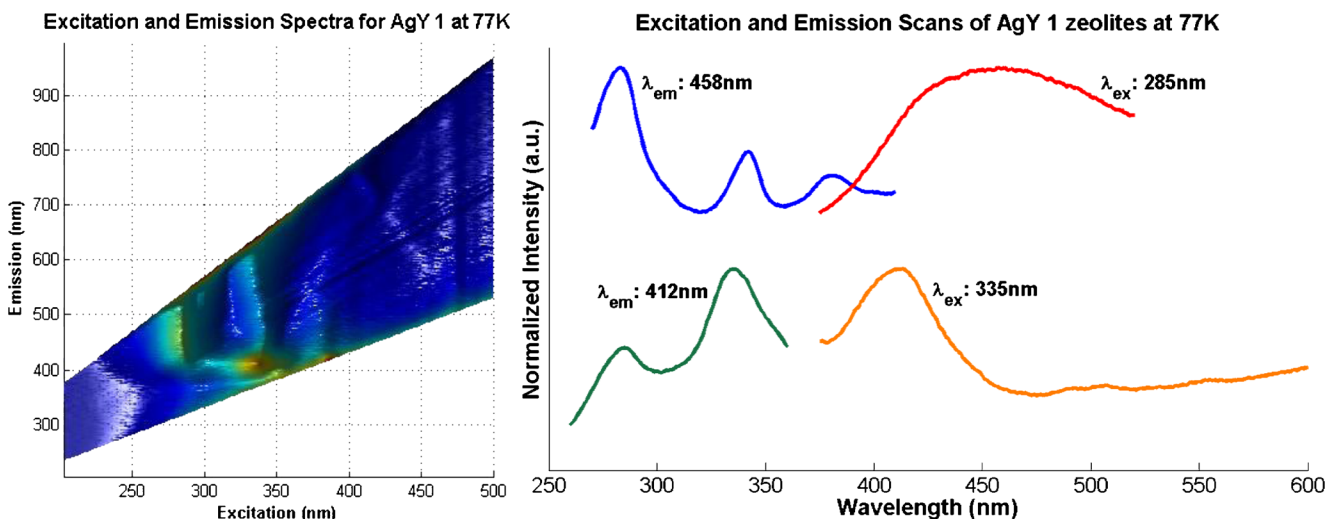

Fig. 2 *Left* 3D excitation/emission matrix scan of AgY1 performed at 77 K. *Right* 2D excitation and emission scans of AgY1 recorded at 77 K
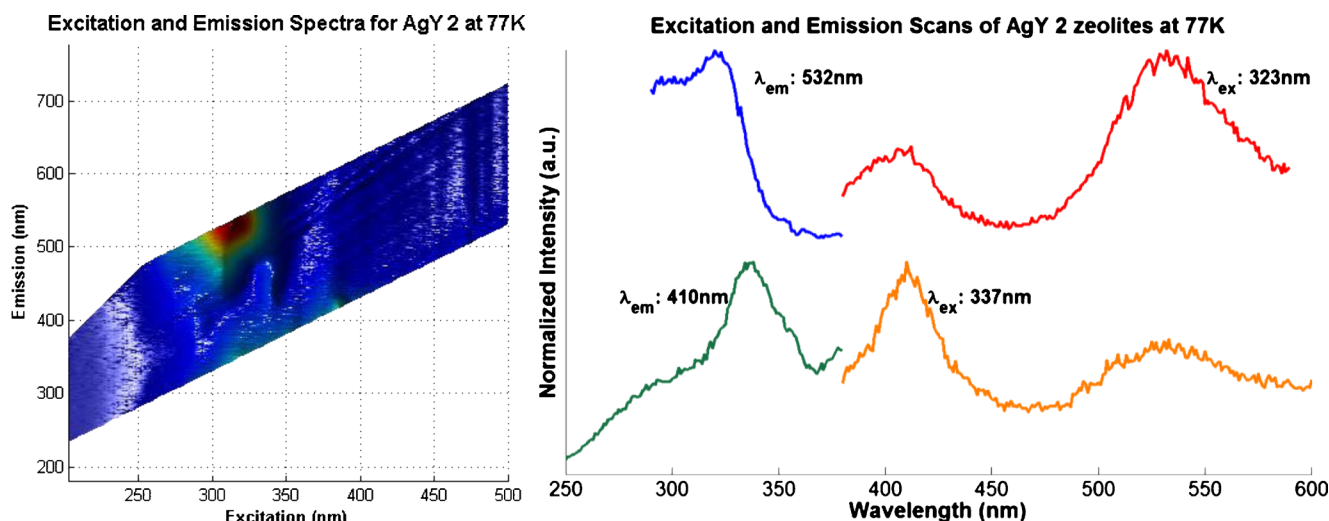
Fig. 3 *Left* 3D excitation/emission matrix scan of AgY2 performed at 293 K. *Right* 2D excitation and emission scans of AgY2 recorded at 77 K

are associated with the LE emission bands and the low-energy excitations are associated with the HE emission bands. Monitoring the energy gap (or Stokes shift when expressed in cm^{-1}) between the excitation and emission energies can be helpful in understanding photophysical interactions within a compound. The Stokes shifts associated with the LE emissions are between 12,200 and 13,500 cm^{-1}, whereas the Stokes shifts for the HE emissions are between 5,280 and 5,580 cm^{-1}. The large Stokes shift for the LE emission band is a result of the large distortion of the silver cluster in its excited emitting state in comparison to its ground electronic state. This distortion allows for shorter Ag-Ag internuclear distances in the excited state from which emission occurs in comparison to the ground electronic state. The decreased Ag-Ag internuclear distance strengthens bonding, thereby stabilizing the excited emitting state.

Stokes shifts such as those between 12,200 and 13,500 cm^{-1} must correspond to a $d^{10} \rightarrow d^9 p^1$ or a $d^{10} \rightarrow d^9 s^1$ electronic configuration change and are assigned to a low-energy observed emission as we have reported for nitrogen-based nucleophiles with copper iodide (Safko et al. 2012). However, Stokes shifts between 5,280 and 5,580 cm^{-1} are assigned to

Ag-Ag transitions within the $[Ag]_3$ trimer. The HE bands around 410 nm are likely a result of direct excitation of linear silver trimers on the interior of the zeolite (Patterson et al. 2007). Whereas, the LE bands observed at 532 to 458 nm in AgY2 and AgY1, respectively, likely appear from delocalized silver clusters $[Ag]_n$ (where $n > 3$) on the surface of the zeolite (Patterson et al. 2007). The difference in emission maxima between the low energy bands in the AgY1 and AgY2 samples is brought on by the formation of different sized silver clusters on the surface of the zeolites. The smaller the silver cluster, the higher the energy of emission (Baril-Robert et al. 2010; Welch et al. 2011; Li et al. 2012). Following this logic, the higher energy emission for AgY1 versus AgY2 can be explained by the higher silver concentration inducing many more small clusters to form on AgY1 than on the AgY2 sample. The LE band is much wider in the AgY1 sample because the higher silver concentration on AgY1 allows for more delocalized clusters of different sizes to form that have slightly different emission energies. Unlike the LE emission band, the position of the HE emission band did not

Table 1 Observed emission maxima for the zeolites at 77 K. The excitation/emission combinations are made by matching similar peak energies

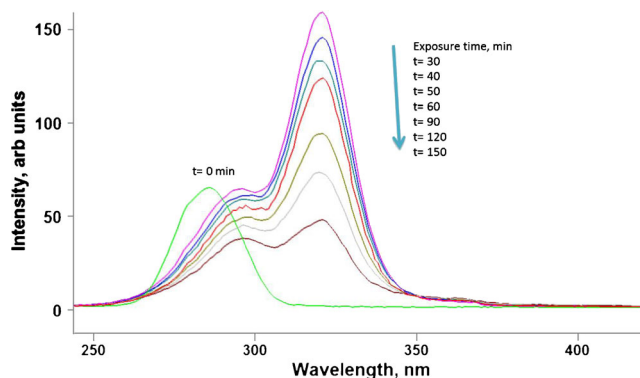| Compound	T (K)	λ^{max}_{em} (nm) [λ_{ex} (nm)]	Stokes shift (cm^{-1})	Transition assignment
AgY1	77	458 [285]	13,300	Delocalized exciplexes
	77	412 [335]	5,580	$[Ag^+]_3$, linear
AgY2	77	532 [323]	12,200	Delocalized exciplexes
	77	410 [337]	5,280	$[Ag^+]_3$, linear

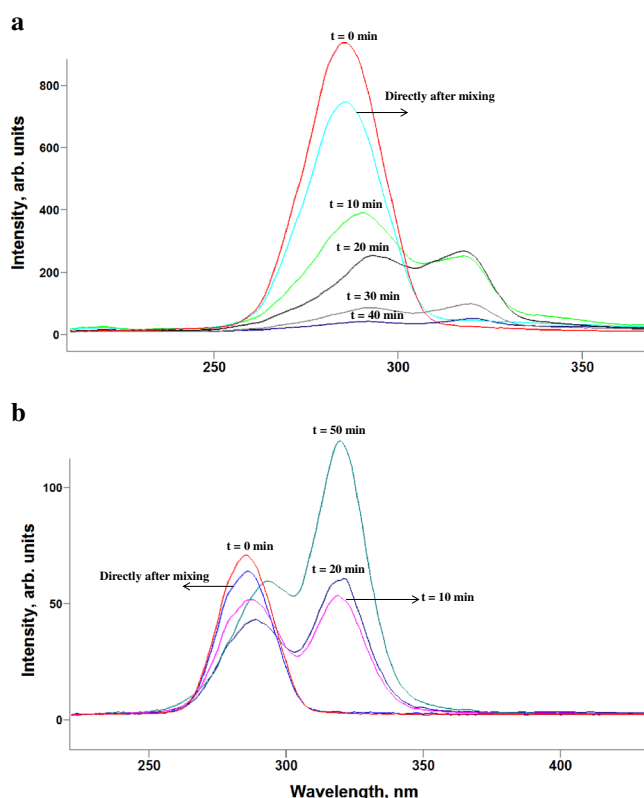**Fig. 4** SSLS of fenoxycarb before and after the irradiation with 254 nm UV light for various time

a

b

Fig. 5 SSLS of fenoxycarb irradiated with 254 nm UV light in the presence of the catalysts **a** AgY1 and **b** AgY2
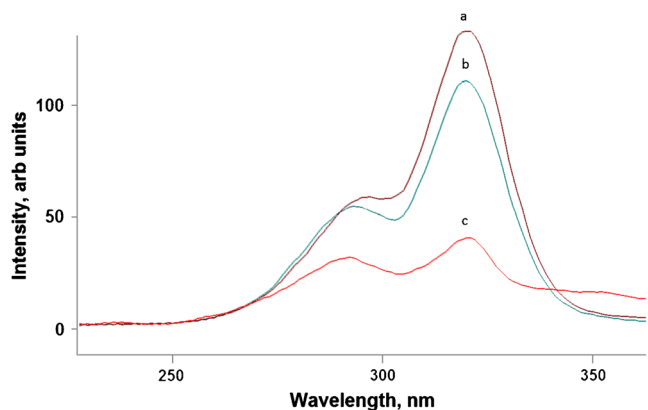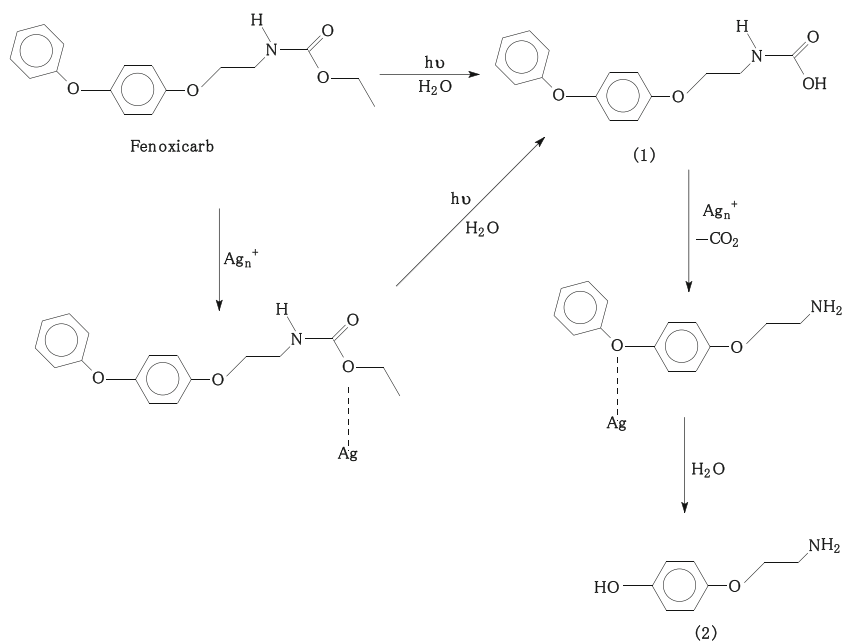

Fig. 6 SSLS of fenoxycarb irradiated for 50 min with 254 nm UV light **a** without a catalyst and the in the presence of **b** AgY2 and **c** AgY1 catalysts

excitation and emission spectra highlighting the two most prominent excitation/emission pairs. Table 1 highlights the excitation/emission maxima and their associated transition assignments for Figs. 2 and 3.

Due to the observed changes in the two catalysts especially in the silver loadings and the tendency to have more Ag-Ag aggregates (delocalized exciplexes) in the high silver sample (AgY1), we expect to observe a change in the catalytic activities. The photodecomposition of fenoxycarb alone and in the presence of the two AgY catalysts was investigated upon UV irradiation. In this study, steady-state luminescence and synchronous scan luminescence spectroscopy (SSLS) along with HPLC were used to monitor the changes occur on the fenoxycarb aqueous solution as a function of irradiation time. Upon excitation at 270 nm, an emission band was observed, with a maximum intensity at 321 nm. This emission is due to the intense π-π^* transition that the pesticide emits at the given energy.

vary much between AgY1 and AgY2. This is likely because the formations of interior linear clusters are not as sensitive to changes in silver concentration.

Figures 2 and 3 have the 3D excitation/emission matrix scans for each zeolite showing all peaks as well as 2D

Scheme 1 Weakening and eventual dissociation of the intramolecular fenoxycarb bonds caused by fenoxycarb-Ag bond

SSLS which involves scanning the excitation and emission wavelength drives of a fluorescence spectrometer simultaneously with a constant wavelength difference between them. This technique is more selective than ordinary fluorescence methods for the analysis of fluorescing mixtures (Kanan et al. 2011). Figure 4 shows the SSLS (with $\Delta\lambda = 30$ nm) of a 30-ppm fenoxycarb solution before (labeled as $t = 0$) and after the exposure of 254 nm UV light for several periods of time. Fenoxycarb initial solution shows a broad band at 285 nm. This band is directly shifted to appear at 295 nm after the irradiation for 10 min along with a new strong band that appears at 325 nm with both bands observed a gradual decrease in their intensity with further irradiation. Interestingly, the photocatalytic behavior of fenoxycarb is different in the presence of the AgY support. Figure 5 shows the SSLS of fenoxycarb irradiated in the presence of AgY1 (Fig. 5a) and in the presence of AgY2 samples (Fig. 5b). As can be seen in Fig. 5, both samples tend to adsorb part of the fenoxycarb from the solution directly upon mixing. In specific, the AgY2 sample adsorbs 12.3 % of the fenoxycarb, while AgY1 adsorbs 20.8 %. In addition, the 285-nm peak does not observe the same shift that appears directly in the uncatalyzed reaction (Fig. 4). This indicates that the presence of the silver zeolite stabilizes the carbamate functionality where silver tends to bind to the carbamates' oxygen (Scheme 1). The AgY1 catalyst (high silver content) has more silver sites that facilitate the adsorption process and thus enhances the photodegradation of the pesticide as seen in Fig. 5a. Silver(I) is an unreactive closed shell d^{10} ion in its ground state but can be excited to a reactive, open shell d^9s^1 or d^9p^1 state (Patterson et al. 2007). In a previous study, we have shown that when nitric oxide reacts with silver(I) in its d^9s^1 excited electronic state, a strong bond forms between the nitric oxide and silver, resulting in a weakening of the N-O bond and its dissociation into nitrogen and oxygen molecules (Kanan et al. 2000). Here, we propose that when the carbamate fenoxycarb reacts with silver(I) in its excited electronic state, strong bonding occurs, forming a strong bond between the two. This new fenoxycarb-Ag bond causes a weakening and eventual dissociation of the intramolecular fenoxycarb bonds (see Scheme 1). The SSLS of the fenoxycarb irradiated with 254 nm for 50 min with and without the AgY samples are presented in Fig. 6. As can be seen in Fig. 6, the decomposition of the pesticide is significant in the presence of AgY1 catalyst, whereas the uncatalyzed reaction shows less degradation.

SSLS along with HPLC and GC-MS spectroscopic techniques were used to characterize the photodecomposition products. HPLC and GC-MS spectra were recorded for the catalyzed and uncatalyzed fenoxycarb solutions that were exposed to the 254 nm UV light for 60 min. Besides the fenoxycarb peak that appears after 2.32 min, two major bands were recorded after 1.58, 1.25 min in the uncatalyzed and the AgY2 catalyzed samples. The AgY1 sample shows only one HPLC band after 1.25 min. Based on the 2.32 min peak areas before and after the irradiation process, the amount decomposed was also calculated. The uncatalyzed sample shows that 58 % of the initial fenoxycarb was decomposed, whereas the decomposition of fenoxycarb in the presence of AgY1 and AgY2 catalysts was 80 and 64 % complete, respectively. Knowing that the maximum amount of silver loaded into the zeolite Y was reached in sample AgY1 (an optimal turn over), a complete decomposition of the pesticide may occur with higher temperatures, longer irradiation time, or by varying the irradiation wavelength/energy of the UV source (Kanan et al. 2007). The products were identified upon the degradation of fenoxycarb for both catalyzed and uncatalyzed experiments using GC-MS. Three GC bands appear after 8.11, 18.7, and 20.3 min. The mass spectrum of the 20.3 min peak indicates the presence of the fenoxycarb, whereas the mass analysis for the 18.7 peak indicates the formation of 2-(4-phenoxy-phenoxy)ethyl] carbamic acid (**1**) (m. mass 273 amu). The peak observed after 8.11 min has a mass of 153 amu, indicating the formation of 1-amine-2-(phenoxy-4-ol) ethane (compound (**2**)).

Conclusion

Silver incorporated into the zeolite Y framework has once again proven capable of reducing the level of pesticide in an aqueous solution. In this study, the presence of the maximum amount of silver loaded on the zeolite decomposes fenoxycarb by 80 % after UV irradiation for 1 h into one product, compound (2). This is a marked increase over UV irradiation alone which reduced fenoxycarb concentration by only 58 % in the same time frame. Future work will focus on examining the relationship between silver cluster structure and the catalytic activity in the presence of dissolved organic carbon to mimic the conditions of natural water systems.

References

Baril-Robert F, Li X, Welch DA et al (2010) Site-selective excitation of "exciplex tuning" for luminescent nanoclusters of dicyanoargentate (I) ions doped in different alkali halide crystals. J Phys Chem C 114: 17401–17408

Escola JM, Aguado J, Serrano DP et al (2011) Catalytic hydroreforming of the polyethylene thermal cracking oil over Ni supported hierarchical zeolites and mesostructured aluminosilicates. Appl Catal B Environ 106:405–415. doi:10.1016/j.apcatb.2011.05.048

Gomez RS, Li X, Yson RL, Patterson HH (2011) Zeolite-supported silver and silver–iron nanoclusters and their activities as photodecomposition catalysts. Res Chem Intermed. doi:10.1007/s11164-011-0313-z

Hernández-Maldonado AJ, Yang RT (2003) Desulfurization of liquid fuels by adsorption via π complexation with Cu(I)-Y and Ag-Y zeolites. Ind Eng Chem Res 42:123–129

Kanan SM (2000) Study of argenate, dicyanoargenate, and dicyanoaurate clusters doped in zeolites and the photoassisted degradation of NOx, malathion, carbofuran, and carbaryl. University of Maine

Kanan MC (2001) A study of the photodegradation of carbaryl: the influence of natural organic matter and the use of silver zeolite Y as a catalyst. University of Maine, Orono

Kanan SM, Omary MA, Matsuoka M, et al (2000) Characterization of the excited states responsible for the action of silver (I)-doped ZSM-5 zeolites as photocatalysts for nitric oxide decomposition. J Phys Chem B 3507-3517

Kanan SM, Kanan MC, Patterson HH (2001a) Photophysical properties of Ag (I)-exchanged zeolite A and the photoassisted degradation of malathion. J Phys Chem B 105:7508–7516

Kanan SM, Tripp CP, Austin RN, Patterson HH (2001b) Photoluminescence and Raman spectroscopy as probes to investigate silver and gold dicyanide clusters doped in A-zeolite and their photoassisted degradation of carbaryl. J Phys Chem B 105:9441–9448

Kanan MC, Kanan SM, Austin RN, Patterson HH (2003a) Photodecomposition of carbaryl in the presence of silver-doped zeolite Y and Suwannee River natural organic matter. Environ Sci Technol 37:2280–2285

Kanan SM, Kanan MC, Patterson HH (2003b) Photoluminescence spectroscopy as a probe of silver doped zeolites as photocatalysts. Curr Opinion Solid State Mater Sci 7:443–449. doi:10.1016/j.cossms.2004.02.005

Kanan MC, Kanan SM, Patterson H (2003c) Luminescence properties of silver(I)-exchanged zeolite Y and its use as a catalyst to photodecompose carbaryl in the presence of natural organic matter. Res Chem Intermed 29:691–704

Kanan SM, Kanan MC, Patterson HH (2006) Silver nanoclusters doped in X and mordenite zeolites as heterogeneous catalysts for the decomposition of carbamate pesticides in solution. Res Chem Intermed 32:871–885. doi:10.1163/156856706778938437

Kanan SM, Abu Yousef IA, Abdo NM (2007) The photodecomposition of phosmet over UV irradiated silver nanoclusters doped in mordenite zeolite. Appl Catal B Environ 74:130–136

Kanan SM, Abdo N, Khalil M et al (2011) A study of the effect of microwave treatment on metal zeolites and their use as photocatalysts toward naptalam. Appl Catal B Environ 106:350–358. doi:10.1016/j.apcatb.2011.05.039

Li X, Pan Z, Welch DA et al (2012) An unusual luminescent anionic copper(I) system: dicyanocuprate(I) ion in nano and bulky states. J Phys Chem C 116:26656–26667

Liu M, Yang H, Liu H et al (2008) Development of high-performance liquid chromatography and non-aqueous capillary electrophoresis methods for the determination of fenoxycarb residues in wheat samples. J Sci Food Agric 67:62–67. doi:10.1002/jsfa

Luengnaruemitchai A, Naknam P, Wongkasemjit S (2008) Investigation of double-stage preferential CO oxidation reactor over bimetallic Au-Pt supported on A-zeolite catalyst. Ind Eng Chem Res 21:8160–8165

Oda S, Tatarazako N, Watanabe H et al (2005) Production of male neonates in four cladoceran species exposed to a juvenile hormone analog, fenoxycarb. Chemosphere 60:74–78. doi:10.1016/j.chemosphere.2004.12.080

Patterson H, Gomez R, Lu H, Yson R (2007) Nanoclusters of silver doped in zeolites as photocatalysts. Catal Today 120:168–173. doi:10.1016/j.cattod.2006.07.057

Payá P, Mulero J, Oliva J et al (2013) Influence of the matrix in bioavailability of flufenoxuron, lufenuron, pyriproxyfen and fenoxycarb residues in grapes and wine. Food Chem Toxicol 60:419–423. doi:10.1016/j.fct.2013.08.013

Safko JP, Kuperstock JE, McCullough SM et al (2012) Network formation and photoluminescence in copper(I) halide complexes with substituted piperazine ligands. Dalton Trans 41:11663–11674. doi:10.1039/c2dt31241g

Valle B, Gayubo AG, Alonso A et al (2010) Hydrothermally stable HZSM-5 zeolite catalysts for the transformation of crude bio-oil into hydrocarbons. Appl Catal B Environ 100:318–327. doi:10.1016/j.apcatb.2010.08.008

Welch D, Baril-Robert F, Li X, Patterson HH (2011) Luminescence and simulation of mixed metal nanoclusters of dicyanoargentate(I) and dicyanoaurate(I) in alkali halides. Inorg Chim Acta 370:279–285. doi:10.1016/j.ica.2011.01.076